Bypassing V1: a direct geniculate input to area MT

Lawrence C Sincich, Ken F Park, Melville J Wohlgemuth & Jonathan C Horton

Thalamic nuclei are thought to funnel sensory information to the brain's primary cortical areas, which in turn transmit signals afresh to higher cortical areas. Here we describe a direct projection in the macaque monkey from the lateral geniculate nucleus (LGN) to the motion-selective middle temporal area (MT or V5), a cortical area not previously considered 'primary'. The constituent neurons are mostly koniocellular, send virtually no collateral axons to primary visual cortex (V1) and equal about 10% of the V1 population innervating MT. This pathway could explain the persistence of motion sensitivity in subjects following injury to V1, suggesting more generally that residual perception after damage in a primary area may arise from sparse thalamic input to 'secondary' cortical areas.

In primates, the pathway mediating visual perception passes from the retina via the LGN to V1. From V1, output is distributed to a panoply of higher extrastriate cortical areas. Historically, these regions were defined as 'higher' because they were not thought to receive direct geniculate input. In humans, loss of V1 devastates eyesight by cutting off the flow of visual information from the LGN to extrastriate visual cortex. Curiously, patients affected by such lesions manifest residual perception—notably for moving stimuli—which occurs either consciously (Riddoch syndrome)[1,2] or unconsciously (blindsight)[3,4]. This phenomenon has engendered considerable controversy[5], and even skepticism, because it defies conventional ideas about the organization of the visual system.

Area MT is a likely site to mediate the persistent ability to sense motion after damage to area V1. In macaques, the responses of single cells in MT account for perceptual decisions about the direction of moving stimuli[6]. Moreover, such judgments are influenced by electrical stimulation, implying direct participation by MT in the perception of motion[7]. A motion-selective area that is homologous to MT has been located in humans[8] and is vital to motion perception[9]. Because MT receives a substantial direct projection from V1 (refs. 10,11), it has been placed directly above V1 in hierarchical models of the visual system[12,13]. Such models currently provide the basic structural framework for explaining neurological syndromes affecting vision.

The simplest explanation for motion sensitivity in subjects after V1 loss is that a visual pathway exists that bypasses V1 to reach MT. Such a pathway might be sufficient to sustain crude motion perception after destruction of V1. Numerous investigators have sought evidence that the LGN projects directly to extrastriate cortex. Indeed, after tracer injection into V2 and V4, scattered retrogradely filled cells have been described in the LGN[14–18]. In a few studies, a direct projection from LGN to MT has also been reported[15,19,20]. These studies have relied on observations in only a few animals, however, and have been contradicted by negative findings[21–23]. An important technical concern is that the optic radiations pass immediately underneath MT, creating the potential for artifactual labeling of LGN cells by tracer

leakage into the white matter. In addition, MT in macaques is completely buried in the superior temporal sulcus (STS), and it lacks well-defined cytoarchitectonic boundaries. These factors make it challenging to place tracer injections accurately into MT without spillover into surrounding cortical areas. Thus a definitive verdict about the existence of projections from LGN to MT is needed. Settling the issue has become especially desirable because MT and V1 are often cast as 'generic' cortical areas in neuroscience, serving as exemplars for studies of cortical processing, perceptual cognition and even conscious awareness[24,25].

To re-examine this issue, we made anatomically verified injections confined to MT in the macaque monkey. We found a sizable population of retrogradely labeled neurons in the LGN that provide direct input to MT. Immunostaining showed that the majority of these neurons form part of the koniocellular system. Notably, a novel subpopulation was present in the LGN intercalated layers, unrelated to the koniocellular system. Our results indicate that a specialized pathway exists from the LGN to MT, which may carry unique visual signals to the motion area in primates.

RESULTS
Distribution of MT-projecting neurons in the LGN and V1

To establish the existence of a direct projection from the LGN to MT, we used a retrograde tracing technique (with CTB, gold-conjugated cholera toxin B subunit) in conjunction with a method of physically unfolding the cortical tissue to delineate clearly area MT[26]. We also verified that the tracer was deposited exclusively in MT by examining the distribution of retrogradely labeled cells in area V1. To indicate how deeply buried MT is in the STS, we show a lateral view of the right hemisphere of monkey 1 at an early stage in the unfolding procedure (**Fig. 1a**). The STS is opened to reveal the location of a single CTB injection in the posterior bank where MT is situated. We also made an array of injections of a second retrograde tracer, WGA-HRP (wheat-germ agglutinin conjugated to horseradish peroxidase) in area V1. The purpose of these additional injections was to ascertain
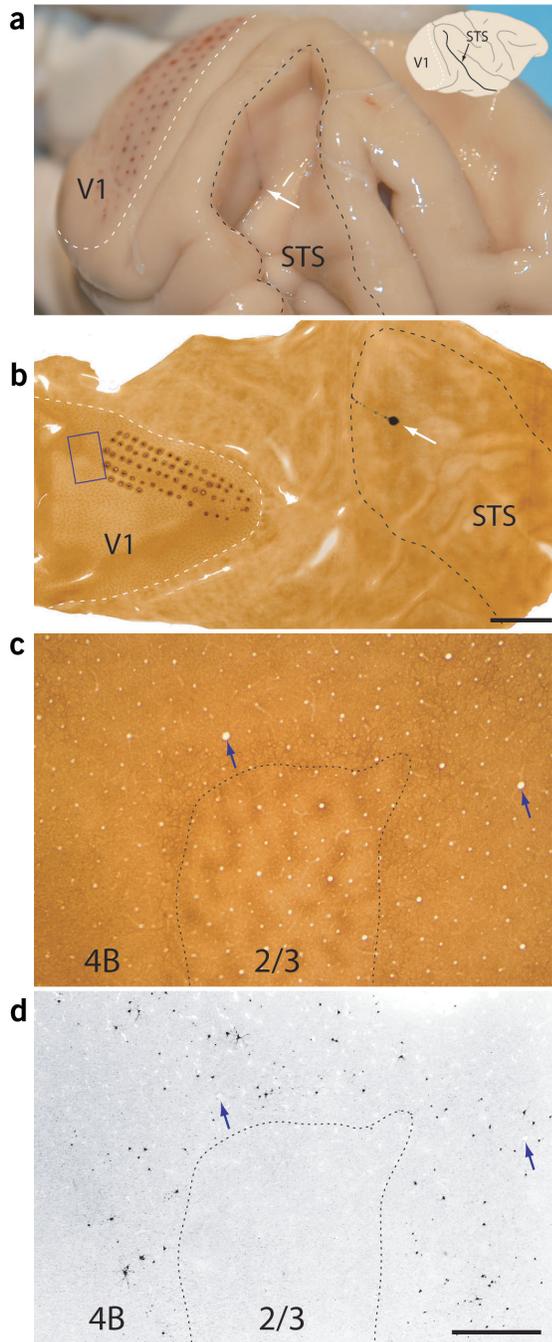
Figure 1 Identifying a tracer injection in MT. (**a**) Lateral view of the right hemisphere of monkey 1 at the start of the flattening procedure, exposing the STS (black dashed outline; inset shows intact view). A CTB injection is indicated by white arrow. Part of V1 (white dashed outline) containing WGA-HRP injections is also visible. (**b**) Single cytochrome oxidase–stained section with WGA-HRP injection sites from an adjacent section superimposed. The CTB injection (white arrow) was centered in a cytochrome oxidase pattern typical of the middle temporal area. (**c**) Higher magnification view from boxed field in **b**, showing the cytochrome oxidase patches of layers 2/3 and the surrounding layer 4B tissue. (**d**) With dark-field illumination of the subjacent section in **c** (image grayscale is inverted), retrograde CTB-labeled cells were visible only in layer 4B. Blue arrows in **c** and **d** indicate blood vessel profiles used for alignment. Scale bars: **b**, 1 cm; **c**,**d**, 1 mm.

STS. The extensive retrograde labeling of neurons in layer 4B of V1 (**Fig. 1c,d**)[27] confirmed that this injection was in MT. We can rule out the possibility that CTB was transported from leakage along the pipette track in adjacent area V4 because there were no CTB-labeled cells in layer 2/3, the only layer in V1 that projects to V4 (ref. 28; **Fig. 1d**).

Additional verification that the injection site was confined to MT was provided by the distribution of retrogradely labeled cells in V1. A density plot of these neurons yielded an island near the middle of V1 (**Fig. 2a**). From this result, one can infer that the tracer injection was made in MT, because projections between V1 and MT unite common retinotopic loci[29]. In both hemispheres of this animal, MT injections were restricted to cortical gray matter, with no contamination of the underlying white matter where tracer might be picked up by fibers of passage (see **Supplementary Fig. 1** online). An example of the V1 labeling pattern from monkey 6, where several CTB deposits were made near the foveal representation in MT, also shows an island of CTB labeling in V1 (**Fig. 2b,c**). It should be noted that where MT-projecting neurons overlapped with the WGA-HRP injections in V1, the CTB cell density was artifactually reduced because the injections tended to obscure CTB-labeled cells. Thus peak cell densities seemed to be displaced away from the WGA-HRP injections, even when the overlap was considerable.

In the corresponding right LGN of monkey 1, we discovered a population of cells that were retrogradely labeled with CTB (**Fig. 3a**). The labeled cells varied in morphology and size, from small stellate and fusiform cells to large multipolar neurons, the latter were among the largest neurons found in the macaque LGN (**Fig. 3b–e,g**). The same pattern of CTB labeling was present in six other LGNs from five additional macaques. When more than one injection was made in MT, as in monkeys 2–6, more labeled cells were found in each LGN section (**Fig. 3a,f**). We examined tissue sections processed for CTB and WGA-HRP to identify double-labeled cells, because their presence would signify that geniculate axons branch before terminating in V1 as well as in MT. Neurons that were the best candidates for double labeling would most likely be found where the fields of CTB and WGA-HRP labeling over-lapped in the LGN. The extent of the overlap varied from animal to animal. For instance, in the LGNs from monkeys 1 and 6, the fields of labeled cells from the two tracers showed more overlap in monkey 6 than in monkey 1 (**Figs. 2** and **3a,f**). Complete searches of overlap areas in the LGNs from four monkeys with coextensive labeling overlap yielded 128 candidate neurons, only 2 of which were double labeled in one LGN of monkey 4. The virtual absence of double-labeled cells indicates that MT-projecting neurons may be a unique population, not merely a subset of V1-projecting neurons with axons that bifurcate and send a branch to MT.

hether axon collaterals of geniculate cells that project to V1 provide the source of input to MT. These WGA-HRP injections are visible as a grid of dots on the posterior pole of the hemisphere (**Fig. 1a**).

Once flattened, the cortical tissue was cut and processed for the metabolic enzyme cytochrome oxidase, a well-established endogenous marker for visual areas. In a single tissue section, three cortical areas were identifiable: V1 by its crisp boundary and cytochrome oxidase patch pattern, V2 by the repeating series of pale-thin-pale-thick stripes encircling V1 and MT by the mottled cytochrome oxidase–rich pattern in the STS (**Fig. 1b**). The WGA-HRP injections were all confined to V1, in a region representing the lower quadrant of the contralateral visual hemifield, covering 0.25–6° from the center of gaze. The CTB injection landed in the characteristic cytochrome oxidase pattern of MT in the
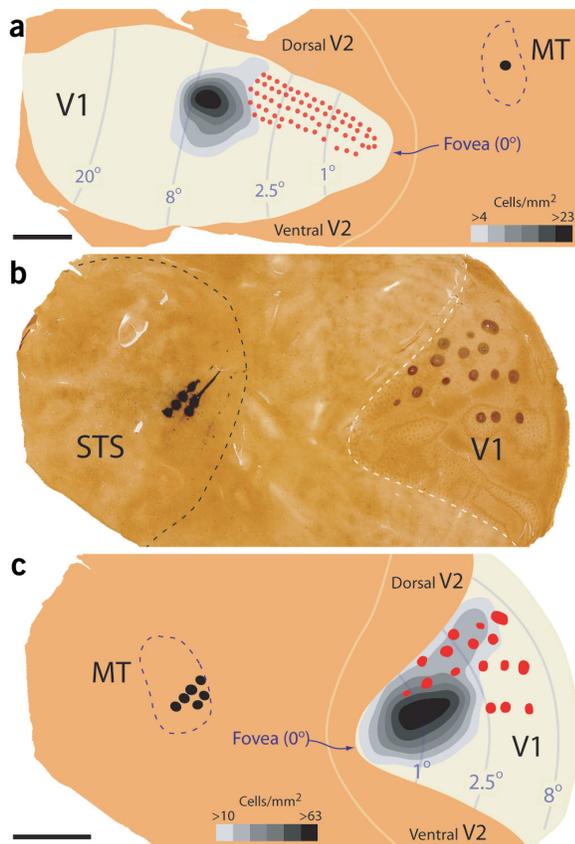
Figure 2 Overlap of MT-projecting neurons and tracer injections in V1. (**a**) CTB-labeled cells found throughout the entire V1 of monkey 1 are depicted as a grayscale density plot. The single island of labeling centered near the 8° eccentricity meridian demonstrated that CTB was injected exclusively in area MT. The grid of WGA-HRP injections is indicated by filled red circles. The nominal border of MT (dashed outline) was estimated from examination of all cytochrome oxidase–stained sections. (**b**) Single cytochrome oxidase–stained section with several CTB injections in MT of the left hemisphere of monkey 6. WGA-HRP injections are superimposed from an adjacent section. In this case, only caudal STS (black dashed outline) and opercular V1 (white dashed outline) were retained. (**c**) V1 CTB labeling for monkey 6, as in **a**, showing extensive overlap of MT-projecting neurons and WGA-HRP injections. Scale bars, 1 cm.

## MT-projecting neurons are part of the koniocellular system

MT-projecting neurons were sprinkled throughout the LGNs of monkey 1, most often in the intercalated layers that are sandwiched between the more prominent parvocellular and magnocellular layers. A similar distribution of labeling was found in four other LGNs in which the location of labeled cells was plotted systematically (**Table 1**). We tested whether these cells were part of the neurochemically distinct koniocellular system that occupies the intercalated layers by immunostaining for the α-subunit of type II Ca^{2+}/calmodulin-dependent protein kinase (CaMK2)[30]. Averaged across all cases, 63% of the CTB-labeled neurons proved to be immunopositive for CaMK2 (**Fig. 4** and **Table 1**). We were surprised to find that these double-labeled cells were present in similar proportions in all layers of the LGN (intercalated, 64%; parvocellular, 65%; magnocellular, 53%).

The distribution of CTB-labeled cells in the LGN had the hallmarks of the koniocellular system, because 70% of the population resided in intercalated layers, with others in the 'bridges' of CaMK2-positive clusters crossing the parvo- and magnocellular layers[30]. The presence of many CTB-positive/CaMK2-negative cells indicated that MT-projecting population was not, however, purely koniocellular. The term koniocellular has been used synonymously with intercalated ever since the first recognition of CaMK2-positive cells in the LGN[30]. Previously, it was impossible to appreciate the heterogeneity of immunostaining within the intercalated layers without a second label to tag other populations. It is now clear that the intercalated layers contain a mixture of cells, some projecting to V1 and others to MT (and still others to V2 and perhaps V4; refs. 14,17,31). One third of the cells within the intercalated layers that project to MT were CaMK2 negative. Therefore, it might be preferable to use 'koniocellular' to refer only to CaMK2-positive cells, without regard to their laminar origin.

Relative retinotopy and population estimate

Comparison of the extent of CTB labeling in the LGN versus V1 allowed us to make two additional observations. First, a single CTB injection in MT labeled a wide field of cells in the LGN, suggesting that the input they provide to MT is retinotopic, but coarser than the input from the LGN to V1. In monkey 1, these cells were distributed throughout half the LGN along the anterior-posterior axis, spanning about 20° of eccentricity in the visual hemifield (approximated from existing LGN retinotopic maps[32]). In contrast, each WGA-HRP injection in V1 produced a small clump of cells in the LGN (**Fig. 3a,f**), representing LGN fields of 2° or less, depending on eccentricity. Notably the retinotopic convergence of the V1 projections to MT was similar. For the same injection in monkey 1, the labeled field in V1 represented approximately 4° of eccentricity in visual space (**Fig. 2a**). Thus, the pathway from LGN to MT provides a retinotopic input that is five or ten times more diffuse than the V1-to-MT or LGN-to-V1 pathways, respectively.

Table 1 Laminar distribution of MT-projecting neurons in CTB- and CaMK2-processed LGN sections

Monkey (hemisphere)	n	CTB only			CTB + CaMK2			Total	Percentage double labeled
		I	P	M	I	P	M		
1 (right)	15	10	8	1	38	4	2	63	70%
1 (left)	18	24	22	4	78	16	0	144	65%
2 (left)	16	61	20	1	103	45	5	235	65%
3 (right)	7	68	11	7	47	8	6	147	41%
4 (left)	7	18	3	1	50	44	3	119	82%
Totals		181	64	14	316	117	16	708	63%

n, number of sections surveyed; I, intercalated; P, parvocellular; M, magnocellular.
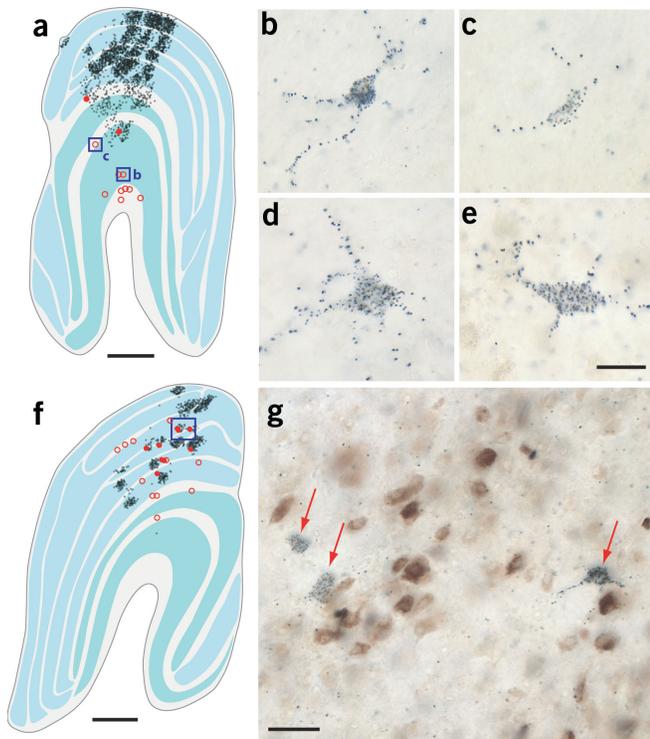
Figure 3 MT-projecting neurons in the LGN. (**a**) Camera lucida plot of the labeled cells in one section of the right LGN of monkey 1. The group of CTB-labeled cells (open and filled red circles) marginally overlaps with the WGA-HRP-labeled neurons (black dots) that project to V1. No double-labeled cells were found in monkey 1. CTB-labeled neurons located within the WGA-HRP field (filled red circles) were considered candidates for double labeling. (**b**–**e**) Photomicrographs from the boxed areas in **a** show that MT-projecting cells vary in morphology, including stellate (in **b**), fusiform (in **c**) and, from the left hemisphere injection of monkey 1, exceptionally large multipolar neurons (in **d** and **e**). (**f**) Camera lucida plot of the left LGN labeling from monkey 6, with extensive overlap between the two tracers. Conventions as in **a**. (**g**) Field from box in **f** showing CTB-labeled cells (red arrows) amid a cluster of WGA-HRP-labeled neurons. (Photographs of the LGN sections are in **Supplementary Fig. 2**.) Scale bars: **a,f**, 1 mm; **b**–**e**, 20 μm; **g**, 30 μm.

MT. The peak V1 labeling of about 60 cells/mm^2, multiplied by an average V1 area of 1,300 mm^2, yields 78,000 MT-projecting neurons in V1. Therefore, assuming only that the LGN and V1 are uniformly populated, a conservative minimum number of MT-projecting cells would be approximately 10% of this number, or about 8,000 cells per macaque LGN. This estimate represents about 1% of the LGN relay neurons. Because these LGN neurons are retinotopically diffuse yet considerable in number, they could provide sufficient wide-field motion information to drive MT in the absence of input from V1.

DISCUSSION

A direct projection from the LGN to MT sheds new light on several puzzling phenomena about the primate visual system. Before discussing these points, it is worth commenting on the fact that most MT-projecting cells are part of the koniocellular system. In the macaque LGN, koniocellular neurons seem to have heterogeneous response properties, although they are most often noted for carrying blue/yellow color signals[33]. MT neurons are capable of detecting motion in isoluminant color stimuli[34,35]. The origin of this color input to MT has, until now, been thought to arise from the mixing of geniculate inputs in V1, where color signals can be passed on to MT from layer 4B or by way of V2 (ref. 36). Presumably, the direct koniocellular input from the LGN also contributes to the color processing abilities of MT.

Second, by calculating the total number of labeled cells in the LGN and in V1 from three hemispheres, we found that the LGN population was numerically equivalent to 10.6% of the V1 population projecting to MT. This proportion was derived from a weighted mean of the neurons counted in the LGN versus V1 (monkey 1R, 126/2,195; monkey 1L, 288/3,460; monkey 2L, 470/2,651). Although it would be valuable to know the total number of LGN cells projecting to MT, this is precluded by the impossible task of injecting the entirety of MT without spillover, and the unknown labeling efficiency of the tracer. An approximation for a lower bound on the population size can, however, be made from an estimate of the total number of V1 layer 4B cells projecting to the

The latency of visual responses in V1 neurons occurs only a few milliseconds earlier, and even occasionally later, than those in MT[37,38]. Although latency studies must be interpreted cautiously[39], such evidence suggests a nearly parallel arrival of initial input. Hierarchical models of the visual system cannot explain such small timing differences because they require at least two synaptic delays for visual signals to pass through V1 to MT (the shortest circuit is LGN→layer 4Cα→layer 4B → MT). Notably, latency studies have consistently found that V2 responses peak after those in MT, even though they would both be subject to similar delays[39]. Given that the quickest signal from the retina to V1 would travel through magnocellular LGN cells, the expected synaptic delays would be 6 ms or more at each stage[38,40,41]. It is difficult to imagine that the very earliest responses of MT are dependent on the input from V1. The pathway we have identified allows visual information to be
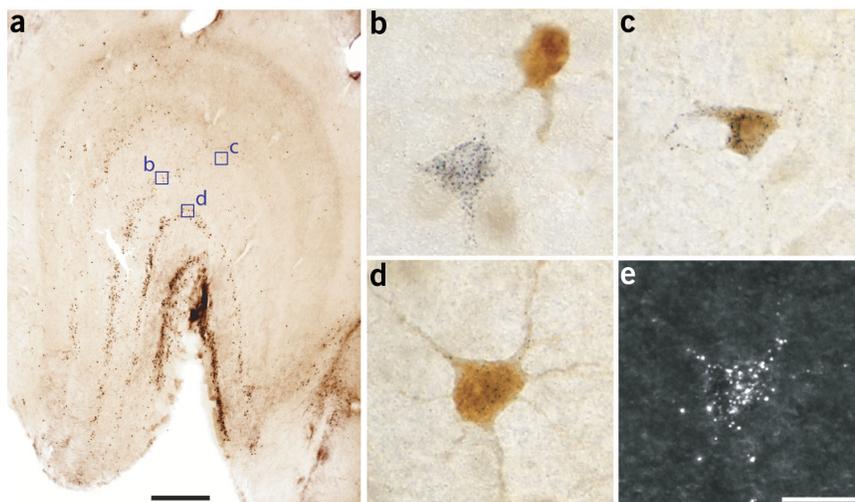
Figure 4 CaMK2 immunostaining of MT-projecting neurons. (**a**) Labeling of the koniocellular layer by CaMK2 in the left LGN of monkey 1. (**b**–**d**) Magnified boxed areas contain a CTB-labeled neuron (**b**, bottom), a CaMK2-positive neuron (**b**, top), and two double-labeled neurons (**c**,**d**). (**e**) Darkfield illumination of the cell in **d** shows the light CTB label. Scale bars: **a**, 1 mm; **b**–**e**, 20 μm.

sent quickly to MT, whereas the koniocellular-dominant character of this input implies that the signal is distinct from those carried by the parvo- and magnocellular channels. A direct pathway from LGN to MT may be especially useful in normal subjects for the rapid detection of moving objects[42].

Our findings also provide some insight into the long-standing controversy about the anatomical underpinnings of blindsight[3]. In both humans and primates with V1 ablation, MT responsiveness is reduced but not eliminated[43–45] (although see ref. 46), and motion perception persists[1,2,5]. Previously, it was assumed that this residual perception was mediated through a variety of subcortical or extrastriate bypass circuits. For example, it was proposed that visual information could reach extrastriate cortex without traversing V1 by going from retina to superior colliculus to pulvinar to MT[47]. Subsequently, however, it was shown that the region of the pulvinar receiving input from the colliculus may possess only a few neurons that project to MT[48]. Perhaps a more promising route through the superior colliculus would be by means of the intercalated layers of the LGN[49].

The existence of a pathway from LGN to MT offers the most straightforward explanation for residual perception of moving stimuli after loss of V1. It also explains why MT responsiveness is completely suppressed during LGN blockade[50]. Our experiments were carried out in macaque monkeys, an Old World primate whose early cortical visual system closely resembles that of humans. It is likely, therefore, that a direct projection from LGN to MT exists in man. The sparseness of the projection agrees with the testimony of blindsight patients who state that they are unconscious of any motion in their blind fields[5]. It remains to be shown physiologically that this pathway can sustain motion perception after loss of V1. It would also be valuable to learn how the direct pathway from the LGN normally influences the response properties of MT cells. Our results show that thalamic nuclei may have a second function beyond relaying signals to primary areas: feeding specialized signals to higher cortical areas. When primary sensory areas are destroyed, the perceptual channels driven by sparse thalamic input may be revealed, giving 'primary' roles to cortical areas traditionally considered to be 'secondary'.

METHODS

Experimental animals and surgical procedures. Six adult male monkeys (three *Macaca fascicularis*, three *Macaca mulatta*) were used, following procedures approved by the UCSF Committee on Animal Research. Anesthesia was induced with ketamine HCl (10 mg/kg, i.m.). The animal was intubated, and anesthesia was maintained with 1.5% isoflurane in a 1:1 mixture of $N_2O:O_2$. We continuously monitored electrocardiogram, respiratory rate, body temperature, blood oxygenation (S_pO_2), endtidal CO_2, and inspired/expired anesthetic gases. A solution of 5% dextrose in 0.45% saline was given intravenously at 3 ml kg^{-1} h^{-1}. After the animal was placed in a stereotaxic frame, a craniotomy and durotomy were made to expose the lunate and superior temporal sulci.

We reconstituted retrograde tracers in filtered, sterile balanced salt solution. For MT injections in all animals except monkey 1, four to six pipette penetrations were spaced 1.5 mm apart laterally along the posterior bank of the STS, beginning 18 mm from the midline. Along each penetration, we made four 120-nl pressure injections of 0.1% CTB (List Biological) every 1.5 mm starting at a depth of 7 mm into the sulcus. In monkey 1, we made a single penetration, depositing CTB at a depth of 8.5 mm. For V1 injections, many 60-nl pressure injections of 4% WGA-HRP (Sigma #L-3892) were made in a 2×2–mm grid pattern in the occipital gyrus, each at a depth of 500 μm. After completing the injections, we sutured the dura and replaced and sealed the bone flap. We repeated the injection series in the other hemisphere. Buprenorphine (0.02 mg/kg, i.m.) was given post-operatively every 8 h until the animal fully recovered.

Histology. After 2 d for transport, the animals were given a lethal dose of pentobarbital (150 mg/kg) and were cardially perfused with 3 liters of 0.9%

saline followed by 1 liter of 1% paraformaldehyde in 0.1 M phosphate buffer. Remaining procedures for CTB and WGA-HRP were as previously described[26]. CaMK2 immunocytochemistry was carried out in floating, agitated, 80-μm-thick sections as follows: (i) two 10-min rinses in PBS, pH 7.4; (ii) 1 h in 10% normal horse serum (NHS) plus 0.2% Triton X-100 detergent in PBS; (iii) two 10-min PBS rinses; (iv) 20–40 h at 8 °C in 1:6,000 anti-CaMK2α mouse monoclonal antibody (MAB8699, clone 6G9; Chemicon) plus 5% NHS and 0.2% Triton X-100 in PBS; (v) four 8-min PBS rinses; (vi) 2 h in biotinylated anti-mouse antibody (Vector Labs) plus 5% NHS and 0.2% Triton X-100 in PBS; (vii) four 8-min PBS rinses; (viii) 1 h in avidin-biotin solution (Vector); (ix) two 5-min PBS rinses and (x) 18 min in 0.05% diaminobenzidine plus 0.01% H_2O_2 in PBS for the chromagenic step.

Data analysis. Cell counts are based on 7 of the 12 LGNs available. In the remaining five cases, CTB-filled cells were present in the LGNs, but the data were rejected because tracer was deposited in the white matter underlying MT or was not confined to MT. LGN sections were surveyed at 400× magnification for all cell counting and camera lucida reconstructions. To compare CTB populations between V1 and the LGN, we estimated the total number of labeled cells from evenly sampled counts. For the LGNs of monkeys 1R, 1L and 2L, we doubled the number of cells from a complete count of every other LGN section. For the corresponding V1s (where sections were cut at 50 μm for cytochrome oxidase and 75 μm for tracer histochemistry), the CTB cells from the thicker series of sections were counted in their entirety. Because this cell count represented 60% of the total V1 tissue volume, the count was multiplied by 1.66 to make the final V1 estimate. Cell density plots in V1 were produced by binning cell counts at a resolution of 2×2 mm in each section and then smoothing the superimposed counts with a gaussian filter ($\sigma = 0.25$ mm). We eliminated two common biases that lead to overestimating cell populations by counting cells in alternate sections and by using sections that are much thicker than the average diameter of the cells being counted.

In searching the LGN for neurons that project to both MT and V1, CTB-labeled cells were considered to be candidates for double labeling only when they resided within clusters of WGA-HRP-labeled cells. CTB-labeled neurons outside the clusters of WGA-HRP labeling were not considered to represent overlapping visual fields and therefore were not included in the analysis.

Note: Supplementary information is available on the Nature Neuroscience website.

1. Riddoch, G. Dissociation of visual perceptions due to occipital injuries, with especial reference to appreciation of movement. *Brain* **40**, 15–57 (1917).
2. Zeki, S. & ffytche, D.H. The Riddoch syndrome: insights into the neurobiology of conscious vision. *Brain* **121**, 25–45 (1998).
3. Humphrey, N.K. & Weiskrantz, L. Vision in monkeys after removal of the striate cortex. *Nature* **215**, 595–597 (1967).
4. Cowey, A. & Stoerig, P. Blindsight in monkeys. *Nature* **373**, 247–249 (1995).
5. Stoerig, P. & Cowey, A. Blindsight in man and monkey. *Brain* **120**, 535–559 (1997).
6. Newsome, W.T., Britten, K.H. & Movshon, J.A. Neuronal correlates of a perceptual decision. *Nature* **341**, 52–54 (1989).
7. Salzman, C.D., Murasugi, C.M., Britten, K.H. & Newsome, W.T. Microstimulation in visual area MT: effects on direction discrimination performance. *J. Neurosci.* **12**, 2331–2355 (1992).
8. Watson, J.D. *et al.* Area V5 of the human brain: evidence from a combined study using positron emission tomography and magnetic resonance imaging. *Cereb. Cortex* **3**, 79–94 (1993).
9. Beckers, G. & Zeki, S. The consequences of inactivating areas V1 and V5 on visual motion perception. *Brain* **118**, 49–60 (1995).
10. Zeki, S.M. The secondary visual areas of the monkey. *Brain Res.* **13**, 197–226 (1969).

ARTICLES

11. Cragg, B.G. The topography of the afferent projections in the circumstriate visual cortex of the monkey studied by the Nauta method. *Vision Res.* **9**, 733–747 (1969).
12. Zeki, S. & Shipp, S. The functional logic of cortical connections. *Nature* **335**, 311–317 (1988).
13. Felleman, D.J. & Van Essen, D.C. Distributed hierarchical processing in the primate cerebral cortex. *Cereb. Cortex* **1**, 1–47 (1991).
14. Yukie, M. & Iwai, E. Direct projection from the dorsal lateral geniculate nucleus to the prestriate cortex in macaque monkeys. *J. Comp. Neurol.* **201**, 81–97 (1981).
15. Fries, W. The projection from the lateral geniculate nucleus to the prestriate cortex of the macaque monkey. *Proc. R. Soc. Lond. B* **213**, 73–86 (1981).
16. Lysakowski, A., Standage, G.P. & Benevento, L.A. An investigation of collateral projections of the dorsal lateral geniculate nucleus and other subcortical structures to cortical areas V1 and V4 in the macaque monkey: a double label retrograde tracer study. *Exp. Brain Res.* **69**, 651–661 (1988).
17. Bullier, J. & Kennedy, H. Projection of the lateral geniculate nucleus onto cortical area V2 in the macaque monkey. *Exp. Brain Res.* **53**, 168–172 (1983).
18. Benevento, L.A. & Yoshida, K. The afferent and efferent organization of the lateral geniculo-prestriate pathways in the macaque monkey. *J. Comp. Neurol.* **203**, 455–474 (1981).
19. Horton, J.C. Cytochrome oxidase patches: a new cytoarchitectonic feature of monkey visual cortex. *Phil. Trans. R. Soc. Lond. B* **304**, 199–253 (1984).
20. Stepniewska, I., Qi, H.X. & Kaas, J.H. Do superior colliculus projection zones in the inferior pulvinar project to MT in primates? *Eur. J. Neurosci.* **11**, 469–480 (1999).
21. Yoshida, K. & Benevento, L.A. The projection from the dorsal lateral geniculate nucleus of the thalamus to extrastriate visual association cortex in the macaque monkey. *Neurosci. Lett.* **22**, 103–108 (1981).
22. Benevento, L.A. & Standage, G.P. Demonstration of lack of dorsal lateral geniculate nucleus input to extrastriate areas MT and Visual 2 in the macaque monkey. *Brain Res.* **252**, 161–166 (1982).
23. Sorenson, K.M. & Rodman, H.R. A transient geniculo-extrastriate pathway in macaques? Implications for 'blindsight'. *Neuroreport* **10**, 3295–3299 (1999).
24. Tong, F. Primary visual cortex and visual awareness. *Nat. Rev. Neurosci.* **4**, 219–229 (2003).
25. Crick, F. & Koch, C. A framework for consciousness. *Nat. Neurosci.* **6**, 119–126 (2003).
26. Sincich, L.C. & Horton, J.C. Independent projection streams from macaque striate cortex to the second visual area and middle temporal area. *J. Neurosci.* **23**, 5684–5692 (2003).
27. Shipp, S. & Zeki, S. The organization of connections between areas V5 and V1 in macaque monkey visual cortex. *Eur. J. Neurosci.* **1**, 309–332 (1989).
28. Yukie, M. & Iwai, E. Laminar origin of direct projection from cortex area V1 to V4 in the rhesus monkey. *Brain Res.* **346**, 383–386 (1985).
29. Ungerleider, L.G. & Mishkin, M. The striate projection zone in the superior temporal sulcus of *Macaca mulatta*: location and topographic organization. *J. Comp. Neurol.* **188**, 347–366 (1979).
30. Hendry, S.H. & Yoshioka, T. A neurochemically distinct third channel in the macaque dorsal lateral geniculate nucleus. *Science* **264**, 575–577 (1994).
31. Rodman, H.R., Sorenson, K.M., Shim, A.J. & Hexter, D.P. Calbindin immunoreactivity in the geniculo-extrastriate system of the macaque: implications for heterogeneity

in the koniocellular pathway and recovery from cortical damage. *J. Comp. Neurol.* **431**, 168–181 (2001).
32. Malpeli, J.G. & Baker, F.H. The representation of the visual field in the lateral geniculate nucleus of *Macaca mulatta. J. Comp. Neurol.* **161**, 569–594 (1975).
33. Hendry, S.H. & Reid, R.C. The koniocellular pathway in primate vision. *Annu. Rev. Neurosci.* **23**, 127–153 (2000).
34. Saito, H., Tanaka, K., Isono, H., Yasuda, M. & Mikami, A. Directionally selective response of cells in the middle temporal area (MT) of the macaque monkey to the movement of equiluminous opponent color stimuli. *Exp. Brain Res.* **75**, 1–14 (1989).
35. Seidemann, E., Poirson, A.B., Wandell, B.A. & Newsome, W.T. Color signals in area MT of the macaque monkey. *Neuron* **24**, 911–917 (1999).
36. Callaway, E.M. Local circuits in primary visual cortex of the macaque monkey. *Annu. Rev. Neurosci.* **21**, 47–74 (1998).
37. Raiguel, S.E., Lagae, L., Gulyas, B. & Orban, G.A. Response latencies of visual cells in macaque areas V1, V2 and V5. *Brain Res.* **493**, 155–159 (1989).
38. Schmolesky, M.T. *et al.* Signal timing across the macaque visual system. *J. Neurophysiol.* **79**, 3272–3278 (1998).
39. Nowak, L.G. & Bullier, J. The timing of information transfer in the visual system. in *Cerebral Cortex* (eds. K.S. Rockland, J.H. Kaas & A. Peters) 205–241 (Plenum, New York, 1997).
40. Maunsell, J.H. & Gibson, J.R. Visual response latencies in striate cortex of the macaque monkey. *J. Neurophysiol.* **68**, 1332–1344 (1992).
41. Nowak, L.G., Munk, M.H., Girard, P. & Bullier, J. Visual latencies in areas V1 and V2 of the macaque monkey. *Vis. Neurosci.* **12**, 371–384 (1995).
42. Cropper, S.J. & Derrington, A.M. Rapid colour-specific detection of motion in human vision. *Nature* **379**, 72–74 (1996).
43. Rodman, H.R., Gross, C.G. & Albright, T.D. Afferent basis of visual response properties in area MT of the macaque. I. Effects of striate cortex removal. *J. Neurosci.* **9**, 2033–2050 (1989).
44. Girard, P., Salin, P.A. & Bullier, J. Response selectivity of neurons in area MT of the macaque monkey during reversible inactivation of area V1. *J. Neurophysiol.* **67**, 1437–1446 (1992).
45. Barbur, J.L., Watson, J.D., Frackowiak, R.S. & Zeki, S. Conscious visual perception without V1. *Brain* **116**, 1293–1302 (1993).
46. Collins, C.E., Lyon, D.C. & Kaas, J.H. Responses of neurons in the middle temporal visual area after long-standing lesions of the primary visual cortex in adult new world monkeys. *J. Neurosci.* **23**, 2251–2264 (2003).
47. Rodman, H.R., Gross, C.G. & Albright, T.D. Afferent basis of visual response properties in area MT of the macaque. II. Effects of superior colliculus removal. *J. Neurosci.* **10**, 1154–1164 (1990).
48. Stepniewska, I., QI, H.X. & Kaas, J.H. Projections of the superior colliculus to subdivisions of the inferior pulvinar in New World and Old World monkeys. *Vis. Neurosci.* **17**, 529–549 (2000).
49. Harting, J.K., Huerta, M.F., Hashikawa, T. & van Lieshout, D.P. Projection of the mammalian superior colliculus upon the dorsal lateral geniculate nucleus: organization of tectogeniculate pathways in nineteen species. *J. Comp. Neurol.* **304**, 275–306 (1991).
50. Maunsell, J.H., Nealey, T.A. & DePriest, D.D. Magnocellular and parvocellular contributions to responses in the middle temporal visual area (MT) of the macaque monkey. *J. Neurosci.* **10**, 3323–3334 (1990).